

Validation of the actuator disc and actuator line techniques for yawed rotor flows using the New MEXICO experimental data

S.-P. Breton¹, W.Z. Shen², S. Ivanell¹

¹Uppsala University Campus Gotland, Cramérgatan 3, 62 157 Visby, Sweden

²Technical University of Denmark, Energivej, Building 414, 2800 Kgs. Lyngby, Denmark

E-mail: wzsh@dtu.dk

Abstract. Experimental data acquired in the New MEXICO experiment on a yawed 4.5m diameter rotor model turbine are used here to validate the actuator line (AL) and actuator disc (AD) models implemented in the Large Eddy Simulation code EllipSys3D in terms of loading and velocity field. Even without modelling the geometry of the hub and nacelle, the AL and AD models produce similar results that are generally in good agreement with the experimental data under the various configurations considered. As expected, the AL model does better at capturing the induction effects from the individual blade tip vortices, while the AD model can reproduce the averaged features of the flow. The importance of using high quality airfoil data (including 3D corrections) as well as a fine grid resolution is highlighted by the results obtained. Overall, it is found that both models can satisfactorily predict the 3D velocity field and blade loading of the New MEXICO rotor under yawed inflow.

1. Introduction

Wind turbines are often operated in conditions where the wind does not flow perpendicularly into the rotor plane, but with a so-called yaw angle. This configuration leads to higher fatigue loads for the rotor blades as well as a more complex development of the flow downstream from the rotor. This configuration being often met in reality, it is important to verify if simulation tools are able to correctly predict the blade loading and velocity field associated to it. Wind tunnel measurements, being performed under controlled inflow conditions, allow to validate simulation methods in this regard. The New MEXICO experiments [1] performed in 2014 in Europe's largest wind tunnel on a three-bladed 4.5m diameter wind turbine will be used here to validate the blade loading and velocity fields under different configurations as predicted using the EllipSys3D Large Eddy Simulation where the rotor plane is modelled using either the actuator disc (AD) or actuator line (AL) model. While both the AD and AL methods in EllipSys3D have recently been used with success to model the New MEXICO rotor under axial inflow [2], the current study will test if they also perform satisfactorily under yawed inflow. Let us mention that yawed inflow has been a subject of investigation for the AL model in EllipSys3D following the first round of the MEXICO wind tunnel experiments [3]. The experimental conditions of the New MEXICO setup differing relatively to the first MEXICO experiment, they allow a further validation of this method.



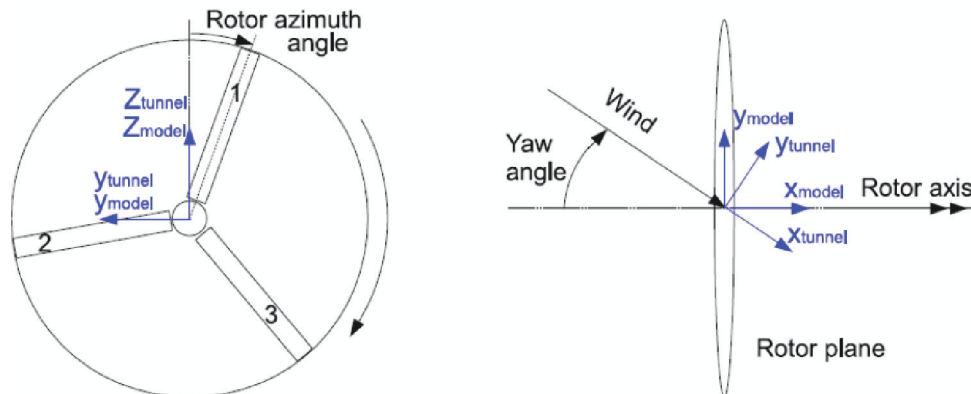


Figure 1. Convention used in the New MEXICO experiments for the coordinate system and yaw angle [4]. Front (left) and top (right) view

In this paper, the numerical and experimental model and setup will first be presented, followed by a presentation and discussion of results regarding the velocity field and blade loading of the New MEXICO rotor under various configurations.

2. Numerical and experimental model and setup

2.1. Experimental setup

The New MEXICO [1] experiments were performed on a three-bladed, 4.5 m diameter upwind wind turbine in the German Dutch Wind Tunnel (DNW). The rotational velocity of the rotor was 425.1rpm, and three incoming velocities (V_0) were considered, i.e. 10.03, 15.01 (design wind velocity) and 24.08m/s. For the case under consideration here, the rotor was yawed at an angle of 30 degrees relative to the incoming flow. Figure 1 [4] illustrates the conventions used for the coordinate system, yaw and azimuth angles. One can see from this figure that a 0 degree azimuth angle corresponds to the reference blade (blade 1) in the vertical position.

The blades were equipped with Kulite pressure sensors, distributed around the airfoil sections at five radial positions, namely at $r/R = 0.25, 0.35, 0.60, 0.82$, and 0.92 , with r the spanwise position, and R the 2.25m radius of the blade. Loads on the blades were calculated as a function of the rotor azimuth angle by integrating the pressure forces around the airfoil section. The blades consisted of three airfoils, namely the DU 91-W2-250 at the root (20 to 45.6 % span), the RISOE A2-21 at the centre of the blade (54.4 to 65.6 % span), and the NACA 64-418 at the tip of the blade (outboard of 74.4% span), with transition zones in between [5]. A cylinder was used from the root (9.3% span) of the blade to 13.3% span. As opposed to the MEXICO first experiments [6], the blades in the current experiments were not tripped with zig-zag strips in the tip region [1].

As in the first MEXICO experiment, the velocity field was also measured in this case, using Particle Image Velocimetry (PIV). The measurements were performed at the 9 o'clock plane relative to the rotor using windows disposed under two configurations and are rotor-phase locked averaged. Under the first configuration, windows were disposed radially in the y_{model} direction shown in Figure 1 to perform so-called radial traverse measurements 0.3m upstream and 0.3m downstream from the rotor plane (i.e. $x_{model} = \pm 0.3m$), leading to results being available for $-3.0m < y_{model} < 3.0m$ for a yaw angle of 30 deg. Under the second configuration, windows

were positioned axially along the x_{tunnel} direction shown in Figure 1 to create axial traverses, whose range covers the interval $-4.5\text{m} < x_{tunnel} < 5.9\text{m}$, leading to results being available at $y_{tunnel} = \pm 1.5\text{m}$ for the same yaw angle. Let us mention that the velocities considered in this work are always defined in the tunnel coordinate system.

While the same spatial resolution as in the first MEXICO measurements was used, the size of the PIV windows increased from 337×394 mm to 380×610 mm in the axial and lateral directions respectively, allowing to cover a larger measurement area. More information about the first and New MEXICO measurement campaigns can be found in [6] and [1] respectively.

2.2. Numerical model and setup

Large-eddy simulations are performed using the Computational Fluid Dynamics (CFD) multi-block finite volume solver EllipSys3D. The rotor is modeled using either the AL or AD technique [7]. Using the AL and AD techniques avoids the need for resolving the development of the boundary layer over the blades, allowing the use of a higher resolution to capture the details of the wake. In the AL model, body forces representing the aerodynamic loads on the rotor are distributed along points on rotating lines representing the individual blades, which allows information about the force on the blades to be directly provided as a function of the blade azimuth angle. In the AD model, the body forces are distributed on points over a rotating disc represented on a local polar mesh, which can provide information about the local forces on the disc as a function of the azimuth angle. The body forces in both techniques are smeared into their imposition points with a three-dimensional Gaussian function [8]. They are calculated through the use of so-called airfoil data, i.e. values of lift and drag coefficients as a function of the local angle of attack, obtained in the LES. Furthermore, the tip loss model by Shen et al. was used in the computations [9, 10].

The airfoil data were obtained from 2D wind tunnel measurements of the RISOE-A1-21 airfoil and provided to the Mexnext participants. It was recently realized that those were not obtained at the right Reynolds number and tripping condition for the RISOE-A2-21 airfoil used in the middle of the blade. However, let us note that the difference in lift-drag polar of the two airfoils is not so different. Work is currently underway to perform measurements under the appropriate conditions. In both the AD and AL simulations, the airfoil data are linearly interpolated in the transition regions between the different airfoil sections. In the AD simulations, the airfoil data associated with a cylinder (i.e., a zero lift coefficient and a value of 1.2 for the drag coefficient) are used for the hub region, while a hole is considered in the AL calculations. Neither the presence of the hub nor of the nacelle is modelled in the EllipSys3D simulations.

The grid used in the AD and AL simulation is the same in order to make a fair comparison possible. It is made up of about 11.8 million points and covers the range $[-20R, 20R] \times [-16R, 16R] \times [-16R, 16R]$ in the x , y and z directions respectively, with the finest resolution given by $R/40$. More information regarding the numerical setup for the calculations performed with the AD and AL models can be found in [2].

3. Results and discussion

An overview of the available simulated and experimental results in terms of velocities in the wake and blade loading, representative of the overall results obtained, is provided and discussed in this section.

3.1. Velocities in the wake

Velocities shown are averaged over the last fourth of the simulations performed with the AD, while the velocities at the last simulation iteration are shown for the AL. Please note that the uncertainty on the experimental velocities, although not included in the graphs, is reported to be around $\pm 0.2\text{m/s}$ [11].

Figure 2 shows the axial (u , along x), crosswise (v , along y) and vertical velocities (w , along z) on the radial traverses located respectively 0.3m upstream and downstream from the rotor in the model coordinate system. Results are shown for the LES using the AD and AL representations of the rotor and are compared to the experimental results. The AD results are shown, upstream from the rotor, to slightly underestimate the downwash effect from the turbine wake as seen in the overestimated axial velocity. It is seen to also underestimate to a certain extent the velocity deficit in terms of axial velocity downstream from the rotor. The AL performs better in this sense and produces results closer to the experimental data. Both the AL and AD simulations compare rather well with the experimental results in terms of crosswise and vertical velocities. The AL and AD results also agree quite well, except for small differences in the hub region due to their different treatment of this region.

Figure 3 shows the same quantities as Figure 2, but for an incoming velocity of 15.01m/s. Observations similar to those related to an incoming velocity of 10.03m/s can be made here. The crosswise velocity which was slightly overestimated upstream from the rotor with the AD model at $V_0=10.03\text{m/s}$ for negative y values is so in a more important way here, and so is the underestimation of the vertical velocity as predicted by the AL model downstream from the rotor for positive y values. Let us notice that the discrepancies observed are similar for these two wind speeds when non dimensionalized with respect to the incoming wind speed. They could result from the use of a slightly too coarse mesh and uncorrected 2D airfoil data.

Figure 4 shows the same quantities as the two previous figures, but for an incoming velocity of 24.08m/s. It is to be noted here that experimental values were available for comparison only for negative y values. In this region, the agreement of both the AD and AL results with the experimental data is quite satisfactory, except for a slight overestimation of the the crosswise velocity component for the AD model both upstream and downstream from the rotor.

The three velocity component as simulated with the AL and AD models and measured experimentally along the axial traverse located at $y_{\text{tunnel}}=-1.5\text{m}$ as a function of the axial position x_{tunnel} are shown in Figure 5 for the three incoming wind velocities considered in the experiments. In all cases shown, it can be observed that both the results associated to the AL model agree quite well with the experimental data. This model is in general able to predict the velocity variations obtained in the experimental data due to the presence of the tip vortices, although with a smaller amplitude. Indeed, for the 10m/s and 15m/s cases, the fine fluctuation details associated to the vertical velocity observed in the experimental data are not reproduced by this AL simulation, while more large variations are produced at a wind velocity of 24m/s [12]. It is expected that the use of a finer resolution mesh would have allowed to reproduce such detailed features of the flow at lower wind velocities, as has been observed before [13]. The AD model, due to its average nature, cannot reproduce these features, but is able to predict the average behavior in the flow quite satisfactorily. Slight overestimations are however obtained as regards the axial velocity downstream from the rotor for incoming velocities of 10.03 and 15.01m/s.

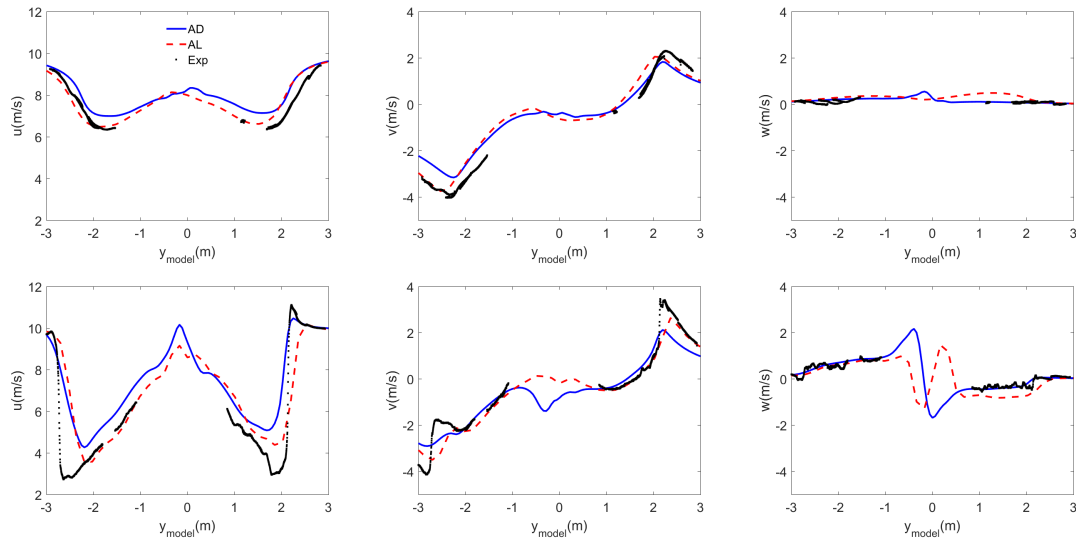


Figure 2. Streamwise, crosswise and vertical wind velocities obtained using the AD and AL in EllipSys3D compared with experimental data. $V_0=10.03\text{m/s}$, yaw angle=30deg, 0.3m upstream (top figures) and downstream (bottom figures) from the rotor plane.

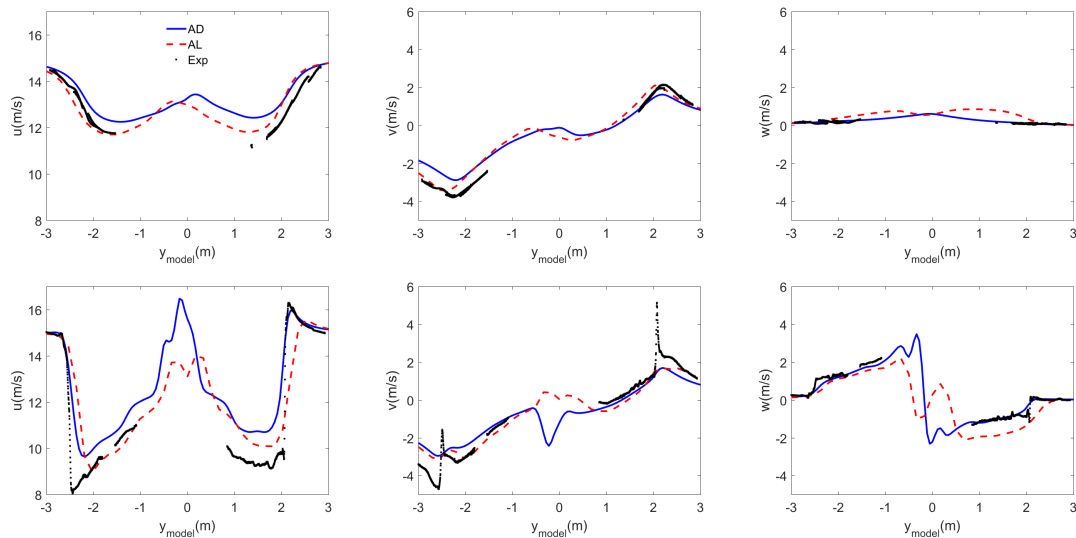


Figure 3. Streamwise, crosswise and vertical wind velocities obtained using the AD and AL in EllipSys3D compared with experimental data. $V_0=15.01\text{m/s}$, yaw angle=30deg, 0.3m upstream (top figures) and downstream (bottom figures) from the rotor plane.

The AL and AD method used in this work, although they do not explicitly model complex phenomena such as flow detachment, which is more important for increasing incoming wind velocities, are shown to be able to satisfactory reproduce the main flow features. Since the structures of the flow, as tip vortices, move more slowly at low incoming velocities, the use of a finer resolution at low wind velocities is expected to lead to a better reproduction of the details of the flow [13].

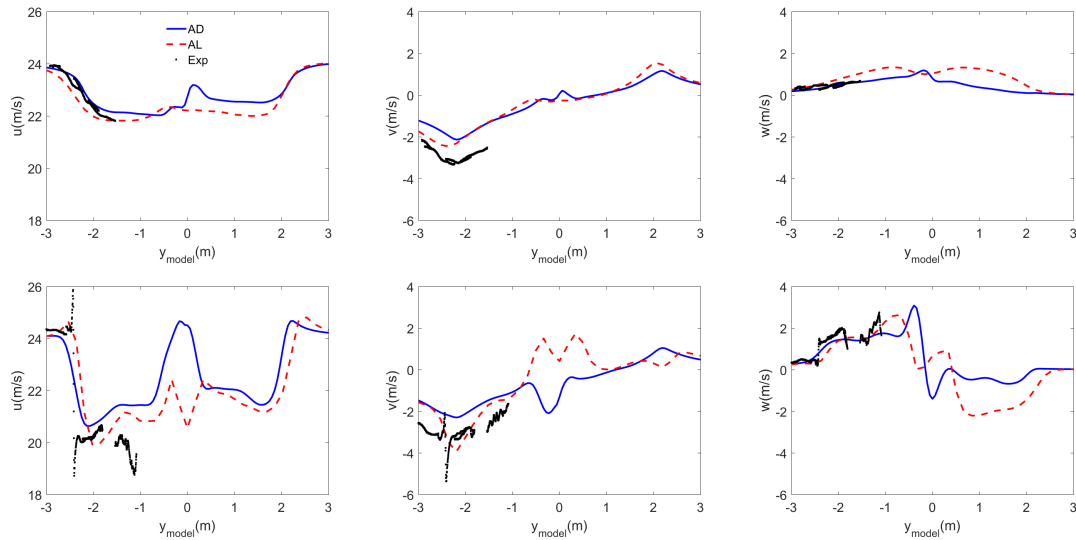


Figure 4. Streamwise, crosswise and vertical wind velocities obtained using the AD and AL in EllipSys3D compared with experimental data. $V_0=24.08\text{m/s}$, yaw angle=30deg, 0.3m upstream (top figures) and downstream (bottom figures) from the rotor plane.

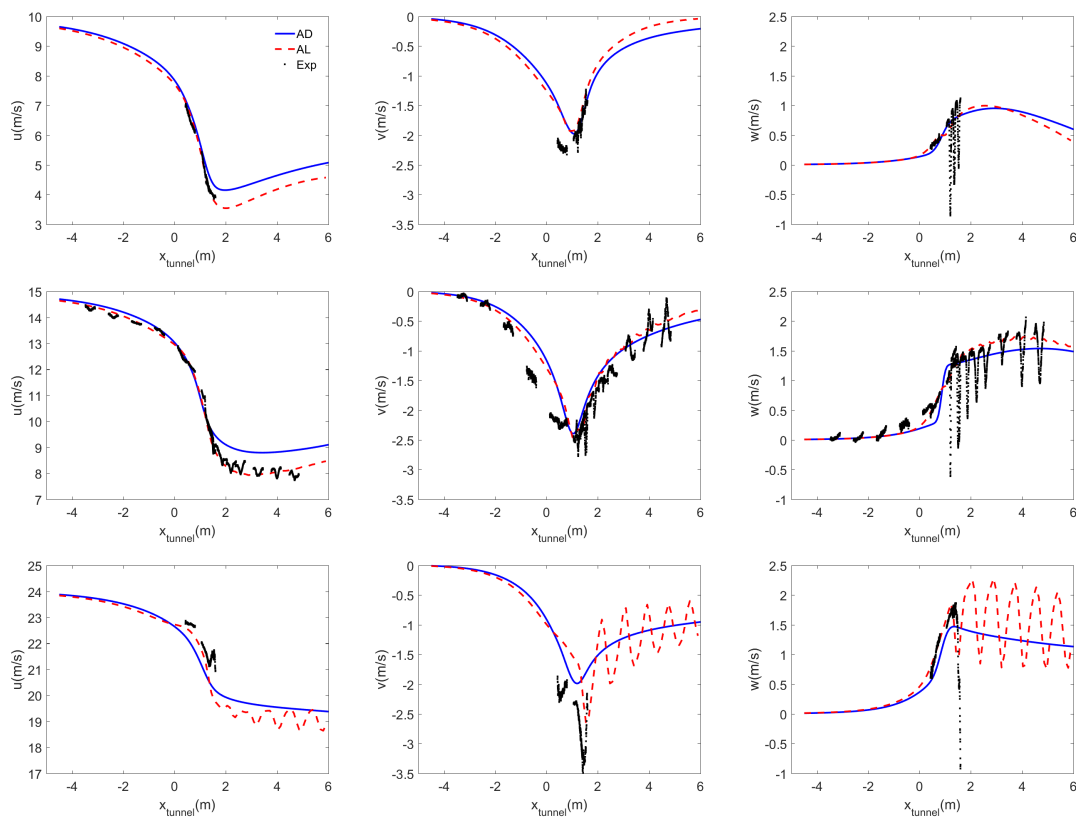


Figure 5. Streamwise (u), crosswise (v) and vertical (w) wind velocities obtained using the AD and AL in EllipSys3D compared with experimental data for the axial traverse located at $y=-1.5\text{m}$. $V_0=10.03\text{m/s}$ (top), 15.01m/s (middle), and 24.08m/s (bottom).

3.2. Blade loading

Figure 6 shows the force normal to the blade chord as simulated using the AD and AL models and measured experimentally the three incoming velocities of 10.03, 15.01 and 24.08m/s. Four positions along the blade representative of the root, center and tip are considered. In general, the AD and AL simulations produce very similar results, and they capture well the azimuthal trend of the normal force. The normal forces are seen to be slightly underestimated in the root region, which is expected to be due to the use of 2D airfoil data which neglect stall delay effects. 2D airfoil data were used in the computations performed within the Mexnext consortium to prevent the use of various 3D correction models that would make a direct comparison between the simulation codes more difficult. Note however that the maximal uncertainty on the force at that position is rather large. The largest differences in terms of amplitude of the forces are seen at a radial position of $0.6R$, near the middle of the blade. These differences could be explained by the fact that the experimental airfoil data used in this section to represent the RISOE airfoil section were not available at the correct Reynolds number and tripping conditions, which could lead to incorrect force values to be computed. The best overall agreement is found for the $0.82R$ position for which the complex influence the tip, known to be difficult to accurately model, is not as important as for the $0.92R$ position.

Figure 7 shows the force tangential to the local blade chord measured and obtained using the AD and AL models for the same radial positions and incoming velocities as in Figure 6. Once again, the AD and AL models lead to very similar results, and are able to reproduce in a satisfactory way the experiments results in terms of trends and absolute values (notice the much smaller y-axis range than for the normal force shown in Figure 6). The tangential force is found to be slightly underestimated in both the AD and AL cases in the root region, which can be explained, as for the normal force, by the neglect of stall delay effects. The differences as regards the amplitude of the tangential force observed at a radial position of $0.6R$ could, as for the normal force, be explained by the issue outlined above regarding the RISOE airfoil in this region. One can notice an interesting feature of the measured tangential force at a radial position of $0.6R$, which does not show the same azimuthal trend as for the other velocities and radial positions. This is expected to result from dynamic stall effects affecting the yawed turbine at this high incoming velocity, a phenomenon that is not specifically accounted for in the current simulations. It would be interesting to investigate whether full CFD simulations modeling in detail the development of the boundary layer over the blades would reproduce this flow behavior.

4. Conclusion

Simulations of the New MEXICO rotor tested under controlled conditions in a wind tunnel were performed under yawed inflow with the Large Eddy Simulation code EllipSys3D, where the disc was modelled using either an actuator disc (AD) or actuator lines (ALs). Comparisons in terms of loading and velocity field with experimental data were made under various configurations. Satisfactory agreement was in general obtained between the experiments and simulations. As regards the velocities, the AL, as expected, was shown in general to be able to capture the induction effect from the individual blade tip vortices, however with a smaller amplitude for low incoming velocities. Although not able to capture this effect, the AD was shown to be capable of reproducing the averaged flow in the near wake quite satisfactorily. It would be interesting in a next step to model the geometry of the nacelle and hub under yawed inflow. This was recently performed under axial flow using both the AD and AL [2] and shown to improve the agreement of the near wake in the blade root region.

The general trends in blade loading were well captured with both the AD and AL models. Small differences were obtained in terms of force amplitude, which were explained by the non-modelling

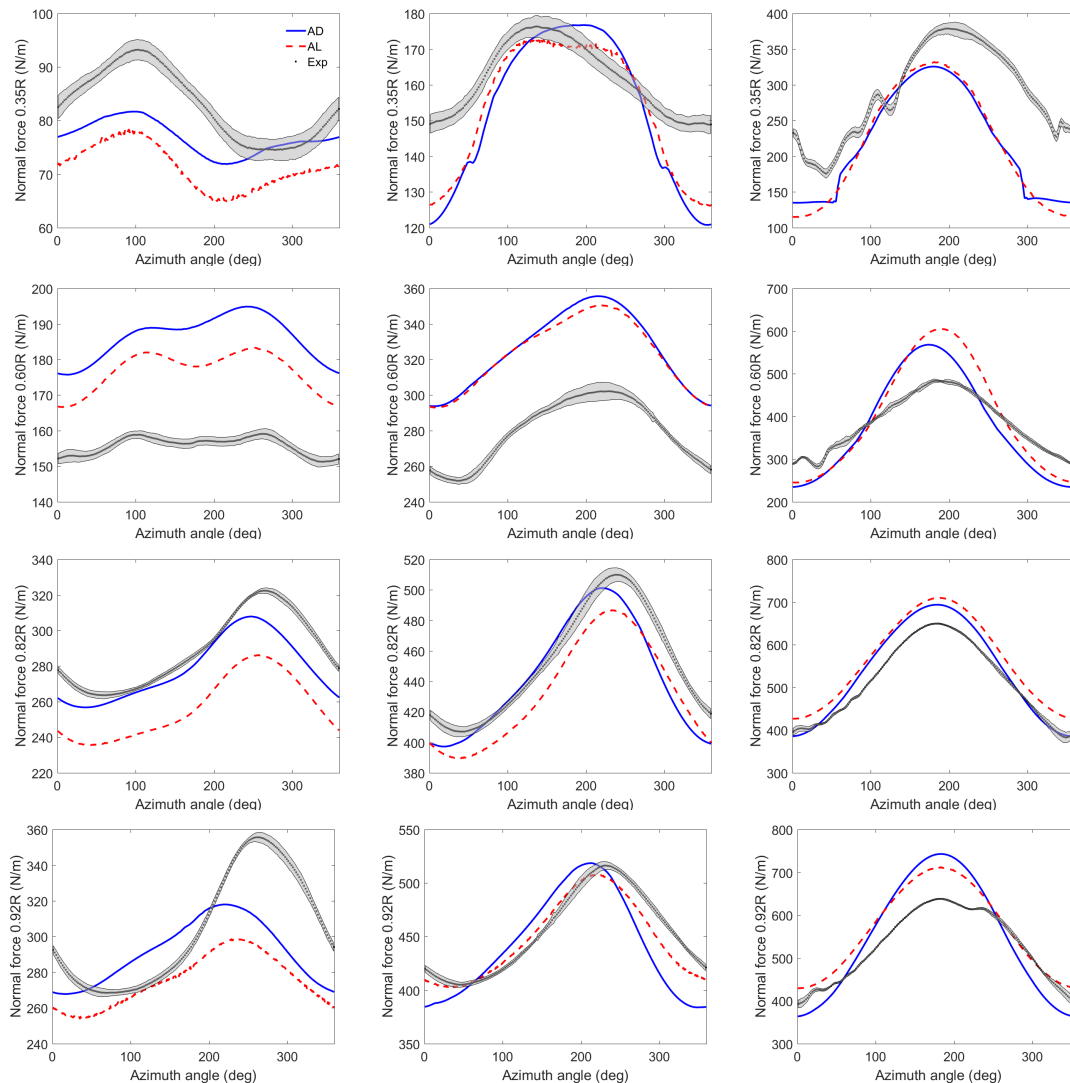


Figure 6. Force per unit length normal to the blade local chord at four radial positions, i.e. $0.35R$ (top), $0.6R$ (2nd row), $0.82R$ (3rd row) and $0.92R$ (bottom) as a function of the blade azimuth angle obtained using the AD and AL in EllipSys3D compared with measurement. Three incoming wind velocities are shown, i.e. $V_0 = 10.03 \text{ m/s}$ (left), 15.01 m/s (middle), and 24.08 m/s (right). The shaded area around the experimental curve shows the uncertainty as \pm one standard deviation, indicating the repeatability between the data points.

of stall delay effects in the root region and use of incorrect airfoil data in the middle part of the blade. This emphasizes the importance of employing as accurate airfoil data as possible for such simulations. This is especially true of the tangential force whose small amplitude makes it very dependent on the validity of the airfoil data. The nature of the airfoil data is found to be more important as regards the prediction of the loading on the blade than for that of the velocity field. It would also be of great interest to compare the present simulations with calculations where the full rotor geometry would be considered to see if experimental trends not totally captured by the current simulations could be reproduced. Nevertheless, both the AD and AL model tested in this work, even though they do not model the development of the boundary layer on the blades or the geometry of the hub and nacelle, are shown to be capable of reproducing the main flow

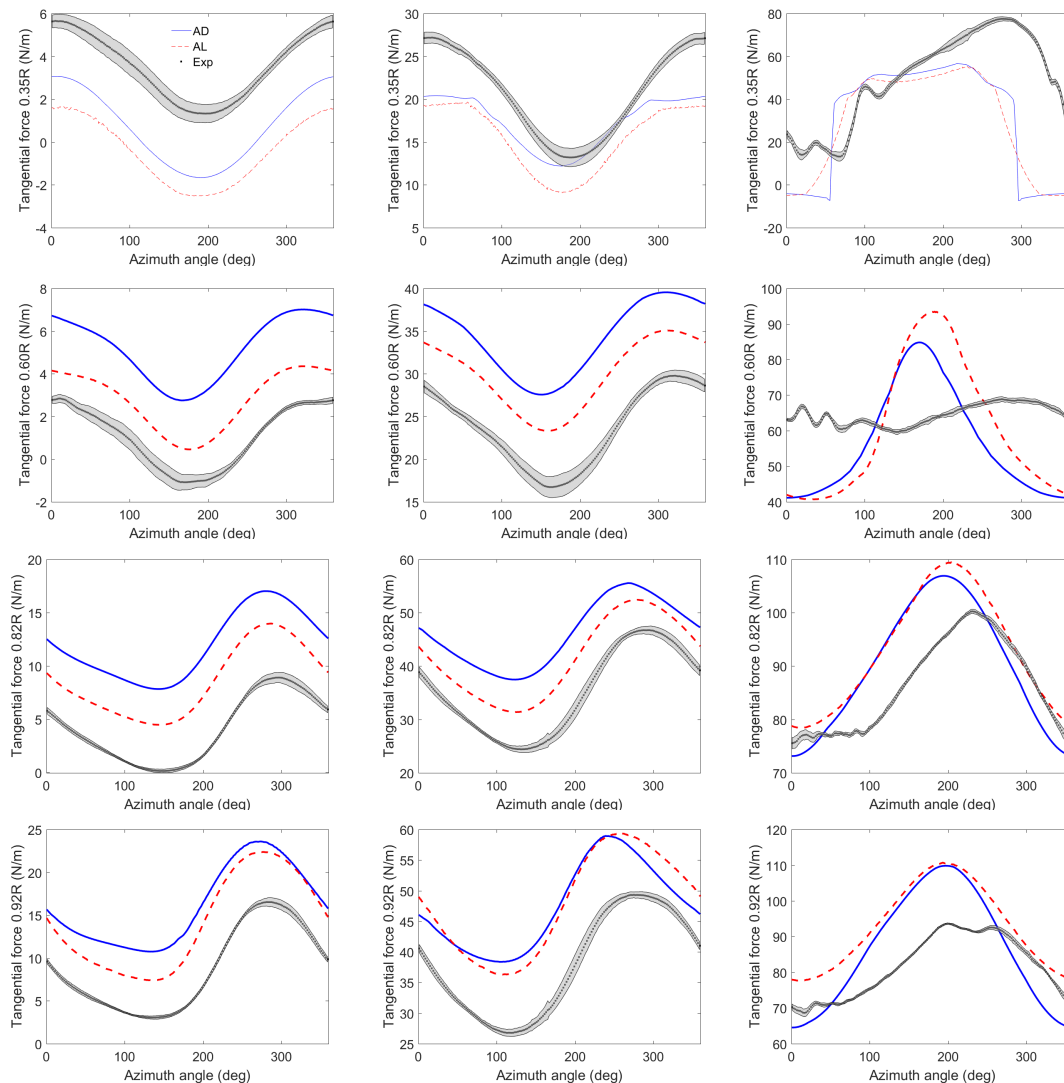


Figure 7. Force per unit length tangential to the blade local chord at four radial positions, i.e. $0.35R$ (top), $0.6R$ (2nd row), $0.82R$ (3rd row) and $0.92R$ (bottom) as a function of the blade azimuth angle obtained using the AD and AL in EllipSys3D compared with measurement. Three incoming wind velocities are shown, i.e. $V_0=10.03\text{m/s}$ (left), 15.01m/s (middle), and 24.08m/s (right). The shaded area around the experimental curve shows the uncertainty as \pm one standard deviation, indicating the repeatability between the data points.

features and blade loading characteristics under yawed inflow.

Acknowledgments

The Swedish Energy Agency is acknowledged for providing research funds for this work. This work was also supported by the Energy Technology Development and Demonstration Program (EUDP2014, J. nr. 64014-0543) under the Danish Energy Agency. The simulations were performed on resources provided by the Swedish National Infrastructure for Computing (SNIC) within the project SNIC 2016/10-33. The authors wish to thank the international partners for their collaborations in the MexNext project coordinated by Energy research Centre of the Netherlands (ECN), within the framework of IEA Task 29. S. Sarmast is acknowledged for help

in setting up the AD simulations.

References

- [1] Boorsma K and Schepers J 2014 New MEXICO experiment - preliminary overview with initial validation. ECN-E-14-048, The Netherlands
- [2] Sarmast S, Shen W, Zhu W, Mikkelsen R, Breton S P and Ivanell S 2016 *Journal of Physics: Conference Series* **753** 032026
- [3] Shen W, Zhu W and Yang H 2015 *Journal of Power and Energy Engineering* **3** 7–13
- [4] Boorsma K and Schepers J 2016 mexnext III: Definition of second round of calculations. Document internal to the Mexnext consortium, ECN, The Netherlands
- [5] Schepers J, Boorsma K, Cho T, Gomez-Iradi S, Schaffarczyk P, Jeromin A, Shen W, Lutz T, Meister K, Stoevesandt B, Schreck S, Micallef D, Pereira R, Sant T, Madsen H and Sørensen N 2012 Final report of IEA task 29, mexnext (phase 1): Analysis of mexico wind tunnel measurements. ECN-E-12-004, The Netherlands
- [6] Schepers J and Snel H 2007 Model experiments in controlled conditions - final report. ECN-E-07-042, The Netherlands
- [7] Sørensen J and Shen W 2002 *Journal of fluids engineering* **124** 393–399
- [8] Mikkelsen R 2003 Ph.D. thesis Technical University of Denmark, Denmark
- [9] Shen W, Mikkelsen R, Sørensen J and Bak C 2005 *Wind Energy* **8** 457–475
- [10] Shen W, Zhang J and Sørensen J 2009 *Journal of Solar Energy Engineering* **131** 011002
- [11] Boorsma K and Schepers J 2015 Description of experimental setup new MEXICO Experiment. ECN-X-15-093-v1, The Netherlands
- [12] Shen W, Zhu W and Sørensen J 2012 *Wind Energy* **15** 811–825
- [13] Nilsson K, Shen W, Sørensen J, Breton S P and Ivanell S 2015 *Wind Energy* **18** 499–514